Available online at www.sciencedirect.com
ScienceDirect
Journal of Sound and Vibration 301 (2007) 846–863
JOURNAL OF SOUND AND VIBRATION
www.elsevier.com/locate/jsvi

Nonlinear vibration analysis for a generic coupled-laminated plate with surface bonded or embedded induced strain actuators

K. Jayakumar[a], D. Yadav[a,*], B. Nageswara Rao[b]

[a]*Department of Aerospace Engineering, Indian Institute of Technology, Kanpur 208016, India*
[b]*Structural Analysis and Testing Group, Vikram Sarabhai Space Centre, Trivandrum 695 022, India*

Received 4 January 2006; received in revised form 22 September 2006; accepted 28 October 2006
Available online 11 December 2006

Abstract

Studies are made on the nonlinear vibrations of Piezo-laminated rectangular thin plates with induced strain actuation by following Kirchoff's hypothesis and using strain-displacement relations of von Kármán type. The von Kármán's large deflection equations for generally laminated elastic plates are derived in terms of stress function and transverse deflection function. A deflection function satisfying the geometric boundary conditions is assumed and a stress function is then obtained after solving the compatibility equation. The modified Galerkin's method is applied to the governing nonlinear partial differential equation to obtain the nonlinear ordinary differential equation of motion (modal equation). This is of Duffing's type. Analytical expressions for the constants in the modal equation are provided to use for any lay-up sequence. Procedure for exact integration of the modal equation is described. Numerical results of simply supported rectangular plates with immovable edges are presented.

1. Introduction

Applications of smart structure technologies to aerospace and other systems are expanding rapidly. Major barriers are: actuator stroke, reliable database of smart material characteristics, non-availability of robust distributed parameter control strategies and reliable mathematical modelling and analysis of smart systems. Among the various smart effects encountered (viz., piezoelectric, electrostriction, magnetostriction, electro-magneto rheological effects and shape memory effects), this paper examines the piezoelectric effect in nonlinear vibrations of thin laminated rectangular plates.

Advanced research is directed towards smart material actuators and sensors [1–3] and piezoelectric, modelling of beams with induced strain actuation [4–10], modelling of plates with induced strain actuation [11–13]. What distinguishes induced strain actuators from conventional hydraulic and electrical actuators and makes them especially attractive for smart structures is their ability to change their dimensions and properties without utilizing any moving parts [14]. These actuator materials contract and expand just like the muscles in the human body. When integrated into a structure (either through embedded or through surface-bonding),

*Corresponding author. Tel.: +91 512 2597951; fax: +91 512 2597561.
E-mail address: dy@iitk.ac.in (D. Yadav).

0022-460X/$ - see front matter © 2006 Elsevier Ltd. All rights reserved.
doi:10.1016/j.jsv.2006.10.024

Nomenclature

a and b	length and width of the plate
A, **B**, **D**	matrices of membrane, coupling, and flexural stiffness of the plate
$f(\zeta)$	restoring force function
h	thickness of plate in z direction
h_i	thickness of ith lamina
h_p	thickness of piezoelectric layer
$I(\zeta)$	potential energy function
M	moment resultants
$\mathbf{M}_\Lambda$	actuator moments
N	stress resultants
$\mathbf{N}_\Lambda$	actuator forces
Q	matrix of reduced stiffness coefficients
$\bar{\mathbf{Q}}$	transformed reduced stiffness matrix
t	time
u, v and w	displacements in x, y and z directions
$W_{mn}(t)$	time dependent amplitude
$\boldsymbol{\varepsilon}$	total strain
$\boldsymbol{\varepsilon}^0$	reference plane strain (i.e., strain at $z = 0$)
ζ	amplitude to thickness ratio
ζ_S	specified amplitude to thickness ratio
$\boldsymbol{\kappa}$	curvature changes
$\boldsymbol{\Lambda}$	actuation strains
ρ_i	density of ith lamina
$\boldsymbol{\sigma}$	stress
φ	Airy's stress function
$\delta\phi_a$	applied electrical potential difference
ω	nonlinear frequency
ω_L	linear frequency

they apply localized strains and directly influence the extensional and bending responses of the structural elements. Because of the absence of mechanical parts they can be easily integrated into the base structure. Integration within the structure ensures an overall force equilibrium between the forcing actuator and the deforming structure, thus precluding any rigid body forces and torques. Using the pin-force model, it was deduced that induced strain actuators, like piezoelectric materials, when bonded to the surface of a structure generate a set of forces, which are concentrated close to the edges of the actuator [15,16]. Therefore, their action is often represented by line moments or forces applied along the periphery of the actuator. This representation simplifies analysis because the structure does not have to be discretized (to represent the non-uniform structural properties in the regions of the patches) and global structural equations can be solved with the actuator forces appearing as discretely applied external forces.

One of the basic elements of adaptive structures is a thin composite plate with surface-induced or embedded sheet actuators. With tailored laminated plate, induced strain actuation can control its extension, bending and twisting. Plates with distributed induced strain actuators can be used: to control pointing of precision instruments in space; to control structural noise; and to change aerodynamic shape for vibration reduction [17], flutter suppression and gust alleviation. Although the pin-force model does not correctly predict the actuator/substrate response for thin structures, it is invaluable in understanding the physics of induced strain actuation. Classical laminated plate theories have been developed to predict flexural response of laminated plates with surface-bonded or embedded induced strain actuators utilizing the advanced models based on assumed strain field [18,19]. Thakkar and Ganguli [20–22] have examined moderate deflections for smart beams and linear applied actuation strain. The effects of actuation strain nonlinearity at high voltages are studied in reference [23].

Two types of nonlinearities are most commonly encountered in plate problems. The geometric nonlinearity arises due to large deformation and material nonlinearity is used to deal with nonlinear material having stress–strain behaviour that is not linear. Librescu [24] and Chia [25,26] provides a wealth of information on a variety of geometrically nonlinear static and dynamic problems of plates. The reviews of Bert [27] and Sathyamoorthy [28] largely deal with the advances made in the analytical methods for solutions of plate problems. For nonlinear free vibration analysis of thin laminated anisotropic plates, the governing equations consists of a system of nonlinear partial differential equations of eighth order in terms of three displacement components (u, v and w) or in terms of the transverse deflection w and force φ. Generally, two methods have been employed in obtaining approximate solutions to such nonlinear problems. These methods are based on the assumptions that the plate deflection is separable in space and time. In the first method, the displacement modes are assumed and the nonlinear partial differential equations are reduced to ordinary differential

equations in time. The law of minimum potential energy states that, of all displacement functions satisfying the boundary conditions, those that satisfy equilibrium conditions give minimum potential energy. There is no guarantee that the assumed displacement modes that satisfy the geometrical boundary conditions will satisfy the equilibrium conditions. Hence, the minimum potential energy obtained by using these displacement modes is not the true minimum [29]. The accuracy of the solution depends on the selection of the displacement modes. The second approach assumes that the deflection time function is sinusoidal when the plate is executing simple harmonic oscillations [30,31].

This paper provides an approximate analytical solution for the nonlinear vibration analysis of piezo-laminated thin rectangular plates by following Kirchoff's hypothesis and using the strain–displacement relations of von Kármán type. A linear model is considered for induced strain in the piezoelectric layer applicable to low fields. The boundary conditions of the plate are simply supported along all the four immovable edges. The von Kármán's large deflection equations for arbitrarily laminated piezo-elastic plates are derived in terms of stress functions and transverse deflection function. The formulation of the theory is based on the fundamental assumption that strains and square of the rotations are small compared to unity. As is well known, the von Kármán plate theory predicts deflections and stresses in a thin plate with reasonable accuracy for deflection having the order of the plate thickness. Thus, the plate theory, which is restricted to small strains but moderately large rotations, is termed as the moderately large deflection theory. A deflection function satisfying boundary conditions is assumed and a stress function is then obtained. Galerkin's method is applied to the governing nonlinear partial differential equations to study the nonlinear vibration characteristics of piezo-laminated thin rectangular plates.

2. Formulation

2.1. System Equations

One of the basic elements of adaptive structures is a thin composite plate with surface-induced or embedded sheet actuators.

A thin rectangular plate of length a in the x direction, width b in the y direction and thickness h, in the z direction is considered (Fig. 1). The z-axis is directed normal to the reference plane ($z = 0$). The thickness of the plate is assumed small in comparison with its smallest lateral dimension (i.e., $h \ll a$ or $h \ll b$). Further it is constructed of an arbitrary number of anisotropic layers, arrangement and thickness. u, v and w are displacements in x, y and z directions, respectively, at the reference plane. The governing equations are based on von Kármán's elastic thin plate theory assumptions. Three additional assumptions are added. First, there is no slip between the adjacent layers of the laminated plate. Second, rotary inertia and transverse shear effects are neglected. Third, kinematics relations, $(\partial u/\partial x)^2$ and $(\partial v/\partial y)^2$are neglected as compared with $(\partial w/\partial x)^2$ and $(\partial w/\partial y)^2$ terms.

Stress resultants and moments provide a simple means of dealing with laminated behaviour. For a generic coupled laminated plate with surface bonded or embedded induced-strain actuators (piezoceramic sheets) placed at arbitrary locations in z direction, the total strain is expressed using the Kirchoff's hypothesis of classical thin plates as

$$\boldsymbol{\varepsilon} = \boldsymbol{\varepsilon}^0 + z\boldsymbol{\kappa}. \tag{1}$$

In view of von Kármán-type geometric nonlinearity, the matrix of strains $\boldsymbol{\varepsilon}^0$ in the reference plane ($z = 0$) is

$$\boldsymbol{\varepsilon}^0 = \begin{Bmatrix} \varepsilon_x^0 \\ \varepsilon_y^0 \\ \varepsilon_{xy}^0 \end{Bmatrix} = \begin{Bmatrix} \frac{\partial u}{\partial x} + \frac{1}{2}\left(\frac{\partial w}{\partial x}\right)^2 \\ \frac{\partial v}{\partial y} + \frac{1}{2}\left(\frac{\partial w}{\partial y}\right)^2 \\ \frac{\partial u}{\partial y} + \frac{\partial v}{\partial x} + \frac{\partial w}{\partial x}\frac{\partial w}{\partial y} \end{Bmatrix}. \tag{2}$$

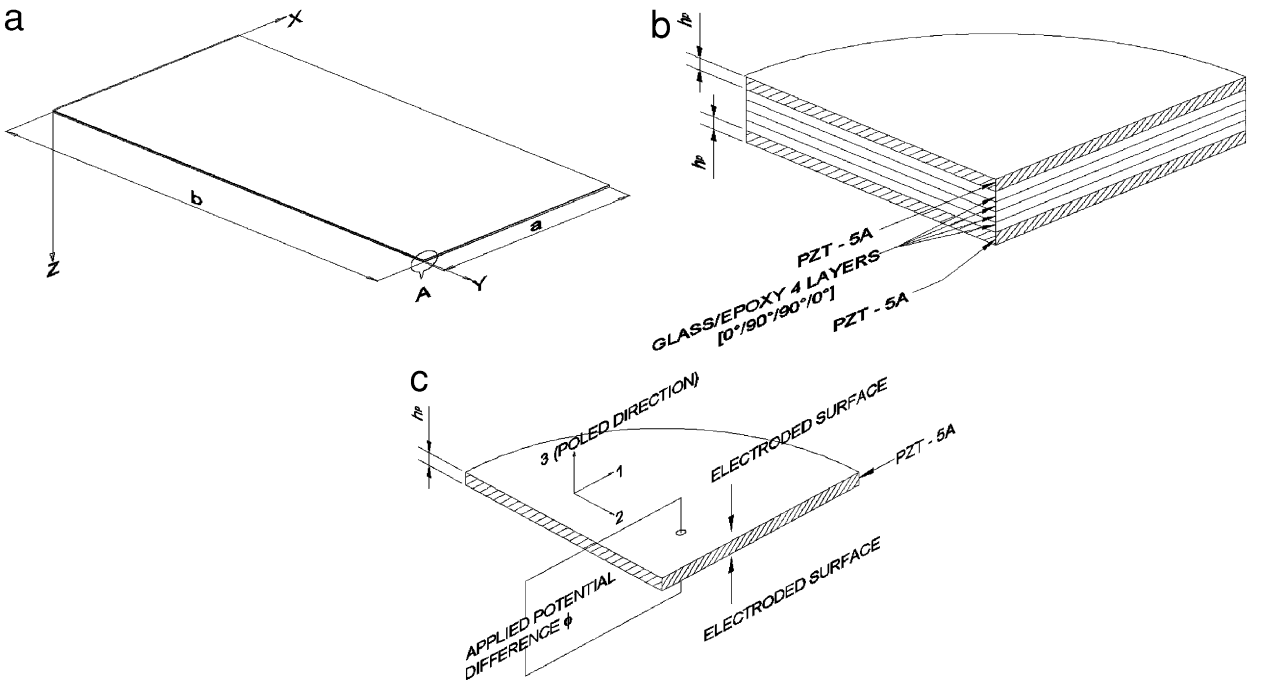

Fig. 1. (a) Overall dimensions of a rectangular plate; (b) the detail at 'A' of (a). A typical smart laminated plate with top and bottom faces with PZT-5A and glass-epoxy as in between layers; and (c) the actuator/sensor layer of the smart plate. The electric field is realized by maintaining a potential difference between the electroded surfaces of the piezoelectric layer.

Assuming small slopes as well as the Kirchoff's hypothesis, the matrix of curvature changes $\boldsymbol{\kappa}$ is

$$\boldsymbol{\kappa} = \begin{Bmatrix} \kappa_x \\ \kappa_y \\ \kappa_{xy} \end{Bmatrix} = -\begin{Bmatrix} \frac{\partial^2 w}{\partial x^2} \\ \frac{\partial^2 w}{\partial y^2} \\ 2\frac{\partial^2 w}{\partial x \partial y} \end{Bmatrix}. \tag{3}$$

The constitutive relation for any ply of a laminated plate is

$$\boldsymbol{\sigma} = \bar{\mathbf{Q}}(\boldsymbol{\varepsilon} - \boldsymbol{\Lambda}), \tag{4}$$

where components in the stress matrix, $\boldsymbol{\sigma} = \{\sigma_x, \sigma_y, \sigma_{xy}\}^{\mathrm{T}}$ and the actuation strain matrix, $\boldsymbol{\Lambda} = \{\Lambda_x, \Lambda_y, \Lambda_{xy}\}^{\mathrm{T}}$. A linear model for induced strain in the piezoelectric layer is utilized in Eq. (4), which is a reasonable approximation at low voltage applicable to low fields. Regarding the modelling of induced strain actuation, proper care is taken while using the constitutive equations for piezoelectric materials, which are "poling-direction" dependent. Referring to Fig. 1, the planar isotropy of poled ceramics is expressed by their piezoelectric strain constants, such that $d_{31} = d_{32}$. The applied static electric field within the piezoelectric actuator is assumed to be constant as the thickness of this layer is relatively small. When an electrical potential difference is introduced across the thickness of the piezoelectric layer (actuator layer), it is strained in its plane. For PZT-5A the in-plane free strain components Λ_x and Λ_y developed in the kth actuator layer, having a charge constant d_{31} and thickness h_p, when an electrical potential difference $\delta\phi_a$ is applied, are

$$\Lambda_x = \Lambda_y = \frac{d_{31}\delta\phi_a}{h_p} \quad \text{and} \quad \Lambda_{xy} = 0.$$

Matrix $\bar{\mathbf{Q}}$ is the transformed reduced stiffness of the plate and $\bar{\mathbf{Q}}\boldsymbol{\Lambda}$ represents an equivalent stress due to actuation. By substituting the assumed deformation into the stress–strain equations and integrating through

the thickness of the plate for net forces and moments, one obtains

$$\begin{Bmatrix} \mathbf{N} \\ \mathbf{M} \end{Bmatrix} = \begin{bmatrix} \mathbf{A} & \mathbf{B} \\ \mathbf{B} & \mathbf{D} \end{bmatrix} \begin{Bmatrix} \boldsymbol{\varepsilon}^0 \\ \boldsymbol{\kappa} \end{Bmatrix} - \begin{Bmatrix} \mathbf{N}_\Lambda \\ \mathbf{M}_\Lambda \end{Bmatrix}. \tag{5}$$

The components in the matrices of the stress and moment resultants, viz., $\mathbf{N} = \{N_x,\ N_y,\ N_{xy}\}^{\mathrm{T}}$ and $\mathbf{M} = \{M_x,\ M_y,\ M_{xy}\}^{\mathrm{T}}$ are defined as

$$(N_k, M_k) = \int_{-h/2}^{h/2} (1, z)\sigma_k \, \mathrm{d}z \quad (k = x, y, xy). \tag{6}$$

N_x, N_y, N_{xy} are membrane forces per unit length, M_x, M_y, M_{xy} are the bending and twisting moments per unit length. The element A_{ij}, B_{ij} and D_{ij} $(i, j = 1, 2, 6)$ in the 3×3 symmetric matrices of **A**, **B**, and **D** in Eq. (5) are defined as

$$(A_{ij}, B_{ij}, D_{ij}) = \int_{-h/2}^{h/2} (1, z, z^2) Q_{ij} \, \mathrm{d}z \quad (i, j = 1, 2, 6). \tag{7}$$

The element A_{ij}, B_{ij}, and D_{ij}, are, respectively, the membrane, coupling and flexural stiffness quantities of the plate. Q_{ij} are the reduced stiffness coefficients. For symmetric anisotropic laminates, the material coupling does not occur between transverse bending and in-plane stretching, viz., $B_{ij} = 0$, whereas in the case of non-symmetric laminated plates $B_{ij} \neq 0$ [24,25].

The components in the matrices of the actuator forces and moments, viz., $\mathbf{N}_\Lambda = \{N_{\Lambda x},\ N_{\Lambda y},\ N_{\Lambda xy}\}^{\mathrm{T}}$ and $\mathbf{M}_\Lambda = \{M_{\Lambda x},\ M_{\Lambda y},\ M_{\Lambda xy}\}^{\mathrm{T}}$ are defined as

$$(N_{\Lambda k}, M_{\Lambda k}) = \int_{-h/2}^{h/2} (1, z) \bar{\mathbf{Q}} \Lambda \, \mathrm{d}z, \tag{8}$$

where

$$\bar{\mathbf{Q}} \Lambda = \sigma_{\Lambda k} = \begin{Bmatrix} \sigma_{\Lambda x} \\ \sigma_{\Lambda y} \\ \sigma_{\Lambda xy} \end{Bmatrix} \quad (k = x, y, xy).$$

Nonlinear equations of motion of generally laminated plates are

$$\frac{\partial N_x}{\partial x} + \frac{\partial N_{xy}}{\partial y} = 0, \tag{9}$$

$$\frac{\partial N_{xy}}{\partial x} + \frac{\partial N_y}{\partial y} = 0, \tag{10}$$

$$\frac{\partial^2 M_x}{\partial x^2} + 2\frac{\partial^2 M_{xy}}{\partial x \partial y} + \frac{\partial^2 M_y}{\partial y^2} + N_x \frac{\partial^2 w}{\partial x^2} + 2N_{xy} \frac{\partial^2 w}{\partial x \partial y} + N_y \frac{\partial^2 w}{\partial y^2} = \sum_{i=1}^{n} \rho_i h_i \frac{\partial^2 w}{\partial t^2}, \tag{11}$$

where ρ_i and h_i are the density and thickness of the ith layer and n is the number of layers in the plate.

The partially inverted form of constitutive equations (5) is written as

$$\begin{Bmatrix} \boldsymbol{\varepsilon}^0 \\ \mathbf{M} + \mathbf{M}_\Lambda \end{Bmatrix} = \begin{bmatrix} \mathbf{A}^* & \mathbf{B}^* \\ -(\mathbf{B}^*)^{\mathrm{T}} & \mathbf{D}^* \end{bmatrix} \begin{Bmatrix} \mathbf{N} + \mathbf{N}_\Lambda \\ \boldsymbol{\kappa} \end{Bmatrix}, \tag{12}$$

where, $\mathbf{A}^* = \mathbf{A}^{-1}$, $\mathbf{B}^* = -\mathbf{A}^{-1}\mathbf{B}$, and $\mathbf{D}^* = \mathbf{D} + \mathbf{B}\,\mathbf{B}^*$.

The Airy stress function φ, which satisfies Eqs. (9) and (10) is defined by

$$N_x = \frac{\partial^2 \varphi}{\partial y^2}, \tag{13}$$

$$N_y = \frac{\partial^2 \varphi}{\partial x^2}, \tag{14}$$

$$N_{xy} = -\frac{\partial^2 \varphi}{\partial x \partial y}. \tag{15}$$

The compatibility equation is derived from relation (2) as

$$\frac{\partial^2 \varepsilon_x^0}{\partial y^2} + \frac{\partial^2 \varepsilon_y^0}{\partial x^2} - \frac{\partial^2 \varepsilon_{xy}^0}{\partial x \partial y} = \left(\frac{\partial^2 w}{\partial x \partial y}\right)^2 - \frac{\partial^2 w}{\partial x^2}\frac{\partial^2 w}{\partial y^2}. \tag{16}$$

Using Eqs. (12)–(15) in Eqs. (11) and (16), one obtains

$$\sum \rho_i h_i \frac{\partial^2 w}{\partial t^2} + L_1(w) + L_3(\varphi) - L(\varphi, w) = 0, \tag{17}$$

$$L_2(\varphi) - L_3(w) - \left(\frac{\partial^2 w}{\partial x \partial y}\right)^2 + \frac{\partial^2 w}{\partial x^2}\frac{\partial^2 w}{\partial^2 y} = 0, \tag{18}$$

where the differential operators are

$$L_1 = D_{11}^* \frac{\partial^4}{\partial x^4} + 4D_{16}^* \frac{\partial^4}{\partial x^3 \partial y} + 2(D_{12}^* + 2D_{66}^*)\frac{\partial^4}{\partial x^2 \partial y^2} + 4D_{26}^* \frac{\partial^4}{\partial x \partial y^3} + D_{22}^* \frac{\partial^4}{\partial y^4},$$

$$L_2 = A_{22}^* \frac{\partial^4}{\partial x^4} - 2A_{26}^* \frac{\partial^4}{\partial x^3 \partial y} + (2A_{12}^* + A_{66}^*)\frac{\partial^4}{\partial x^2 \partial y^2} - 2A_{16}^* \frac{\partial^4}{\partial x \partial y^3} + A_{11}^* \frac{\partial^4}{\partial y^4},$$

$$L_3 = B_{21}^* \frac{\partial^4}{\partial x^4} + (2B_{26}^* - B_{61}^*)\frac{\partial^4}{\partial x^3 \partial y} + (B_{11}^* + 2B_{22}^* - 2B_{66}^*)\frac{\partial^4}{\partial x^2 \partial y^2} + (2B_{16}^* - B_{62}^*)\frac{\partial^4}{\partial x \partial y^3} + B_{12}^* \frac{\partial^4}{\partial y^4},$$

$$L(\varphi, w) = \frac{\partial^2 \varphi}{\partial y^2}\frac{\partial^2 w}{\partial x^2} + \frac{\partial^2 \varphi}{\partial x^2}\frac{\partial^2 w}{\partial y^2} - 2\frac{\partial^2 \varphi}{\partial x \partial y}\frac{\partial^2 w}{\partial x \partial y}.$$

Therefore, Eqs. (17) and (18) are two coupled governing equations of arbitrarily piezo-laminated thin plates.

2.2. Solution approach

The large amplitude vibrations of simply supported generic coupled laminated rectangular plate with surface bonded or embedded induced strain actuators are examined here by applying the Galerkin's method.

Boundary conditions for simply supported rectangular plates are

$$w = 0, \quad M_x = 0 \quad \text{at } x = 0, a, \tag{19}$$

$$w = 0, \quad M_y = 0 \quad \text{at } y = 0, b. \tag{20}$$

The inplane boundary conditions for immovable edges are

$$\int_0^a \left\{ \varepsilon_x - \frac{1}{2}\left(\frac{\partial w}{\partial x}\right)^2 \right\}_{y=0,b} \mathrm{d}x = 0, \tag{21}$$

$$\int_0^a \{N_{xy}\}_{y=0,b} \mathrm{d}x = 0, \tag{22}$$

$$\int_0^b \left\{ \varepsilon_y - \frac{1}{2}\left(\frac{\partial w}{\partial y}\right)^2 \right\}_{x=0,b} \mathrm{d}y = 0, \tag{23}$$

$$\int_0^b \{N_{xy}\}_{x=0,a} \mathrm{d}y = 0. \tag{24}$$

The system of Eqs. (17) and (18) in terms of the transverse deflection w and stress function φ, are to be solved in conjunction with the boundary conditions (19)–(24). A deflection shape function for w satisfying the geometric boundary conditions of the plate is assumed. A stress function φ is then obtained from the compatibility Eq. (18). Galerkin's method is applied to the governing nonlinear partial differential equation to yield a second-order ordinary nonlinear differential equation of motion in time variable. The details of the solution of the problem are briefly described below.

The transverse supporting conditions given in Eqs. (19) and (20) are satisfied by assuming a deflection functions for the laminate in the separable form corresponding to the wavenumbers m, n as

$$w = W_{mn}(t)\,\sin(\alpha_m x)\,\sin(\beta_n y), \tag{25}$$

here,

$$\alpha_m = \frac{m\pi}{a}, \quad \beta_n = \frac{n\pi}{b}.$$

Substituting the transverse deflection, w into the Eq. (18), and solving, utilizing the in-plane boundary conditions, the stress function φ is obtained as

$$\varphi = \varphi_0(x,y) + W_{mn}\varphi_1(x,y) + W_{mn}^2\varphi_2(x,y). \tag{26}$$

The expressions for the functions, φ_0, φ_1 and φ_2 are given in Appendix A. It should be noted that for symmetric anisotropic laminates, the bending-stretching coupling matrix $\mathbf{B} = 0$ and $\mathbf{D}^* = \mathbf{D}$ in Eq. (12). For this case $\varphi_1(x,y)$ as defined in Appendix A vanish and Eq. (26) for Airy's potential is independent of linear term in W_{mn}.

When w and φ are substituted into Eqs. (19) and (20), the force boundary conditions are not satisfied when $\mathbf{B}^*$ does not equal zero. In such a situation usage of the modified Galerkin's method [32] is more appropriate. In the case of simply supported rectangular plates assuming $\bar{w} = \sin\alpha_m x\,\sin\beta_n y$, the residual force and moment have the following relation:

$$\int_0^a\int_0^b L^R(\varphi,w)\bar{w}\,\mathrm{d}x\,\mathrm{d}y + \int_0^b \left(M_x\frac{\partial\bar{w}}{\partial x}\right)_{x=0}\mathrm{d}y + \int_0^b \left(M_x\frac{\partial\bar{w}}{\partial x}\right)_{x=a}\mathrm{d}y + \int_0^a M_y\left(\frac{\partial\bar{w}}{\partial y}\right)_{y=0}\mathrm{d}x + \int_0^a M_y\left(\frac{\partial\bar{w}}{\partial y}\right)_{y=b}\mathrm{d}x = 0, \tag{27}$$

where $L^R(\varphi,w)$ is residual force.

Letting $L^N(\varphi,w) = L^R(\varphi,w) + L(\varphi,w)$, Eq. (17) then becomes

$$\sum_{i=1}^{n}\rho_i h_i\frac{\partial^2 w}{\partial t^2} + L_1(w) + L_3(\varphi) - L^N(\varphi,w) = 0. \tag{28}$$

Applying Galerkin's method to Eq. (27), the modal equation is then obtained as

$$\sum_{i=1}^{n}\rho_i h_i\frac{\mathrm{d}^2 W_{mn}}{\mathrm{d}t^2} + \alpha_\Lambda + \alpha W_{mn} + \beta W_{mn}^2 + \gamma W_{mn}^3 = 0. \tag{29}$$

The constants α_Λ, α, β, γ and δ in the above equation (29) are defined in Appendix B.

For symmetric anisotropic laminates, $\mathbf{B}^* = \mathbf{0}$, which implies that the constant coefficient $\beta = 0$ in the modal equation (29). Hence, the quadratic term in the restoring force function of equation of motion vanish for symmetric laminates.

Defining $\zeta = W_{mn}/h$ and $\tau = \omega t$, the modal equation (29) is written in the form

$$\omega^2\ddot{\zeta} + \omega_L^2 f(\zeta) = 0, \tag{30}$$

where the restoring force function,

$$f(\zeta) = \delta_0 + \zeta + \delta_1\zeta^2 + \delta_2\zeta^3, \tag{31}$$

and

$$\omega_L = \sqrt{\frac{\alpha}{\sum_{i=1}^{n} \rho_i h_i}}$$

is the linear frequency of the plate, $\delta_0 = (\alpha_\Lambda/\alpha h)$, $\delta_1 = (\beta h/\alpha)$, $\delta_2 = (\gamma h^2/\alpha)$ and ω is the nonlinear frequency, and over-dot denotes differentiation with respect to τ.

The initial conditions for Eq. (30) are

$$\zeta = \zeta_s, \quad \dot{\zeta} = 0 \quad \text{at } \tau = 0. \tag{32}$$

Here ζ_s is the ratio of the amplitude of the transverse deflection and the thickness of the plate. The restoring force function $f(\zeta)$ in the equation of motion (30) is a cubic polynomial, which is of Duffing type or a combination of quadratic and cubic terms.

Solution for the nonlinear frequency of the plate, which is a function of material properties, dimensions of the plate and the amplitude of vibration, can be obtained by several methods such as the perturbation method [32] the harmonic balance method [33], the hybrid Galerkin's method [29], exact integration [34] and iterative numerical schemes [35]. Nayfeh and Mook [36] have described some of the conventional tools for the analysis of nonlinear oscillations, such as, averaging techniques, multiple-time scaling and harmonic balancing. In the present study the resulting equation of motion (30) is solved through exact integration.

If $\delta_0 = 0$ and $\delta_1 = 0$, then $f(\zeta)$ becomes an odd function, and the magnitudes of maximum positive and negative amplitudes in the periodic motion will be equal. In the case of mixed-parity (i.e., $\delta_0 \neq 0$ and $\delta_1 \neq 0$), $f(\zeta)$ is a non-odd function and the magnitudes of maximum positive and negative amplitudes in the periodic motion will be different. Hence, for non-odd function $f(\zeta)$ the behaviour of oscillations is different for the positive and negative amplitudes. That means the frequency values for the specified maximum positive and negative amplitudes having the same magnitude, will be different.

The relationship between the positive and negative amplitudes, viz. ζ_+ and ζ_-, can be found by equating the potential energies in either position, i.e. from

$$I(\zeta_+) = I(\zeta_-), \tag{33}$$

where

$$I(\xi) = \int_0^{\xi} f(\eta)\mathrm{d}\eta = \delta_0\xi + \frac{1}{2}\xi^2 + \frac{\delta_1}{3}\xi^3 + \frac{\delta_2}{4}\xi^4. \tag{34}$$

Multiplying Eq. (30) by $\mathrm{d}\zeta/\mathrm{d}\tau$ and integrating,

$$\frac{1}{2}\omega^2\left(\frac{\mathrm{d}\zeta}{\mathrm{d}\tau}\right)^2 + \omega_L^2\{I(\zeta) - I(\zeta_-)\} = 0. \tag{35}$$

The initial conditions used while integrating Eq. (30) to obtain Eq. (35) are

$$\zeta = \zeta_-, \quad \dot{\zeta} = 0 \quad \text{at } \tau = 0. \tag{36}$$

The solution curve on the $\zeta - \dot{\zeta}$ plane is referred as the integral curve or the phase trajectory. In the periodic motion of the system, the solution curve on the $\zeta - \dot{\zeta}$ plane is a closed trajectory. If $\delta_0 = 0$ and $\delta_1 = 0$, $f(\zeta)$ is an odd function and $I(\zeta_+)$ is an even function. The solution curve of Eq. (35) will be symmetric on ζ and $\dot{\zeta}$ axis. If $\delta_0 \neq 0$ and $\delta_1 \neq 0$, the solution curve of Eq. (35) will be symmetric only on the ζ axis.

Integrating Eq. (35) from $\tau = 0$ to $\tau = \pi$, one gets

$$\frac{\omega_L}{\omega} = \frac{1}{\sqrt{2}\pi}\int_{\zeta_-}^{\zeta_+} \frac{\mathrm{d}\zeta}{\sqrt{I(\zeta_-) - I(\zeta)}}. \tag{37}$$

For a specified maximum positive amplitude-to-thickness ratio ζ_+ the corresponding maximum negative amplitude-to-thickness ratio ζ_- is obtained from Eq. (33) and vice versa. By substituting ζ_- and ζ_+ in Eq. (37) the nonlinear frequency ω is obtained. The integrand in Eq. (37) has poles at the end of integration (i.e., at

$\zeta = \zeta_-$ and ζ_+), which may adversely affect the accuracy of an integration rule. Hence, the integrand in Eq. (37), is modified by using

$$\zeta = \zeta_1 + \zeta_2 \cos\left\{\frac{1}{2}\pi(1+\xi)\right\}. \tag{38}$$

That eliminates the singularities and yields a form

$$\frac{\omega}{\omega_L} = \left(\frac{1}{2}\int_{\xi=-1}^{\xi=1} \frac{\mathrm{d}\xi}{\sqrt{c_0 + c_1\zeta + c_2\zeta^2}}\right)^{-1}, \tag{39}$$

where

$$c_0 = 1 + \frac{4}{3}\delta_1\zeta_1 + \frac{1}{2}\delta_2(3\zeta_1^2 + \zeta_2^2), \quad c_1 = \frac{2}{3}\delta_1 + \delta_2\zeta_1, \quad c_2 = \frac{1}{2}\delta_2,$$

$$\zeta_1 = \frac{1}{2}(\zeta_+ + \zeta_-), \zeta_2 = \frac{1}{2}(\zeta_+ - \zeta_-).$$

The negative amplitude-to-thickness ratio ζ_- corresponding to the positive amplitude-to-thickness ratio ζ_+ obtained from Eq. (33) is

$$\zeta_- = \frac{(s_1 + s_2 - a_2)}{a_3}, \tag{40}$$

where

$$s_{1,2} = \sqrt{r \pm \sqrt{q^3 + r^2}}, \quad q = a_3a_1 - a_2^2, \quad r = \frac{1}{2}(3a_3a_2a_1 - a_3^2a_0) - a_2^2,$$

$$a_3 = c_2, \quad a_2 = \frac{1}{3}\left(\frac{2}{3}\delta_1 + a_3\zeta_+\right), \quad a_1 = \frac{1}{3} + a_2\zeta_+, \quad \text{and} \quad a_0 = 3a_1\zeta_+ + 2\delta_0.$$

A ten-point Gaussian rule was adopted while evaluating the integral in Eq. (39).

3. Results and discussions

3.1. Comparison with published results

As the formulation is general, comparison of results for validation are carried out with those that are available in published literature, when piezoelectric layers and induced actuation are absent.

The results presented in Table 1 are found to be in good agreement with those of Chia and Prabhakara [37] and Mei and Umphai [38], obtained by different numerical schemes for isotopic square plates with wavenumbers $m = n = 1$.

The variation of frequency ratio (ω/ω_L) with the amplitude ratio (ζ_S) is shown in Fig. 2 for a rectangular plate ($a/b = 2$; $b/h = 100$) and lay-up sequence: [0°/90°/90°/0°]. The properties used in the analysis are [39]:

Table 1
Frequency ratio (ω/ω_L) for the specified amplitude ratio (ζ_S) of a simply supported isotropic square plate with immovable edges ($a/b = 1$, $b/h = 100$, $E_{11}/E_{22} = 1$, $\nu_{12} = 0.3$, $E_{11} = 2.6G_{12}$)

Amplitude ratio ζ_S	Chia and Prabhakara [37]	Mei and Umphai [38]	Present study
0.2	1.0185	1.0182	1.0195
0.4	1.0717	1.0709	1.0757
0.6	1.1534	1.1530	1.1625
0.8	1.2566	1.2589	1.2734
1.0	1.3753	1.3826	1.4024

Coefficients in the restoring force function (31): $\delta_0 = \delta_1 = 0$ and $\delta_2 = 0.34125$.

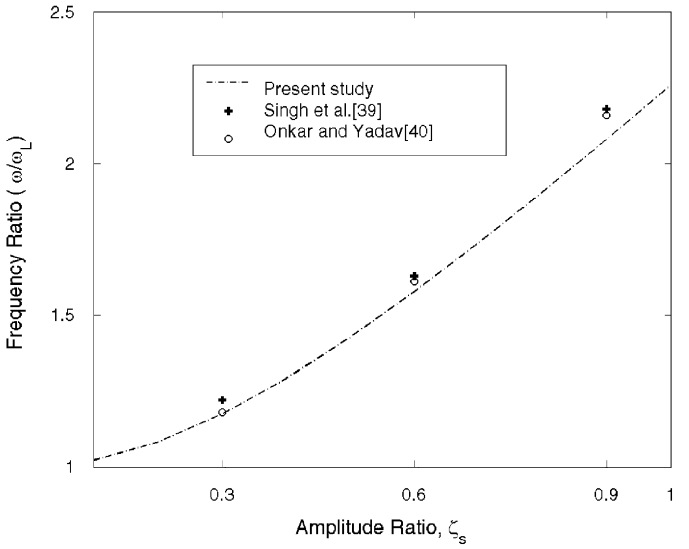

Fig. 2. Variation of frequency ratio (ω/ω_L) with amplitude ratio (ζ_S) for a rectangular laminated plate for $m = n = 1$; $(a/b) = 2$, $(b/h) = 100$; stacking sequence $[0°/90°/90°/0°]$.

Table 2
Material properties considered for glass-epoxy and PZT-5A

Property	Glass-epoxy	PZT-5A
Moduli		
E_{11}	143 GPa	63 GPa
E_{22}	9.7 GPa	63 Gpa
G_{12}	6 Gpa	24.2 Gpa
Poisson's ratio v	0.3	0.3
Density ρ	2000 kg/m^3	7800 kg/m^3
Piezoelectric charge constant d_{31}	—	-154×10^{-12} m/V

$E_{11} = 40E_{22}$, $G_{12} = 0.5E_{22}$ and $v_{12} = 0.25$. The constants in the equation of motion are: $\delta_0 = 0$, $\delta_1 = 0$ and $\delta_2 = 0.3536$. The results obtained by Singh et al. [39] and Onkar and Yadav [40] are found to be reasonably in good agreement with the present analysis.

3.2. Nonlinear frequency

This paper examines the nonlinear free vibration of simply supported piezo-laminated rectangular thin plates with moderately large deflection. Numerical results for simply supported plates with immovable edges are presented for wavenumbers $m = n = 1$. Fig. 1 shows the configuration of the plate considered for the present analysis. The piezoelectric layer can be surface bonded or embedded in one of the layers. The top and bottom layers are composed of PZT-5A. Glass-epoxy laminate is sandwiched between them. Table 2 gives the material properties for glass-epoxy and PZT-5A considered in the present numerical experiment. Piezoelectric materials have the advantage of being used as actuator as well as sensors. The top layer is considered as actuator and the bottom layer acts as the sensor/actuator. The feedback voltage for correcting the error in the required response through the actuator layer is realized by the sensor/actuator layer. The actuation voltage, strains the top layer. This alters the nonlinear vibration behaviour of the laminate. On application of strains of opposite magnitude in the bottom layer, one gets the same response as that of strain-free laminate. It should be noted that the applied strains are within the rated capacity of the PZT-5A. The strength of PZT-5A is 75.9 MPa, the rated stress is 20.7 MPa. Various cases of lamina sequence are considered for a six-layered plate.

Table 3
Coefficients in the restoring force function (31) of equation of motion (30) and linear frequencies for symmetric and anti-symmetric lay-up sequence of a square plate with applied electric potential difference

Applied electric potential difference $\delta\varphi_a$ (Volts)	Stacking sequence [PZT-5A/0°/0°/0°/0°/PZT-5A]		Stacking sequence [PZT-5A/0°/0°/90°/90°/PZT-5A]	
	$\delta_0 = \delta_1 = 0$		$\delta_0 = \delta_1 = 0$	
	δ_2	ω_L(Hz)	δ_2	ω_L(Hz)
Direction of applied electric field is same as poling direction of PZT-5A crystal				
0.0	1.38	749.4	1.43	735.6
400.0	1.42	737.2	1.48	723.1
533.5	1.47	724.8	1.53	710.5
800.0	1.52	712.2	1.59	697.6
1067.0	1.58	699.4	1.65	684.5
Direction of applied electric field is opposite to poling direction of PZT-5A crystal				
−0.0	1.38	749.43	1.43	735.6
−400.0	1.33	761.4	1.39	747.8
−533.5	1.29	773.2	1.34	759.8
−800.0	1.25	784.9	1.30	771.7
−1067.0	1.22	796.3	1.26	783.3

Dimensions of the plate: $a = 100$ mm, $b = 100$ mm, $h = 2.2$ mm, (aspect ratio, $a/b = 1$).
Wave numbers: $m = n = 1$.

Table 4
Coefficients in the restoring force function (31) of equation of motion (30) and linear frequencies for symmetric and anti-symmetric lay-up sequence of a rectangular plate with applied electric potential difference

Applied electric potential difference $\delta\varphi_a$ (Volts)	Stacking sequence [PZT-5A/0°/0°/0°/0°/PZT-5A]		Stacking sequence [PZT-5A/0°/0°/90°/90°/PZT-5A]		
	$\delta_0 = \delta_1 = 0$		$\delta_0 = 0$		
	δ_2	ω_L(Hz)	δ_1	δ_2	ω_L(Hz)
Direction of applied electric field is same as poling direction of PZT-5A crystal					
0.0	1.11	451.2	0.0101	1.81	464.1
400.0	1.18	438.5	0.0107	1.91	451.8
533.5	1.25	425.4	0.0113	2.03	439.0
800.0	1.34	411.8	0.0120	2.16	425.9
1067.0	1.43	397.9	0.0128	2.30	412.4
Direction of applied electric field is opposite to poling direction of PZT-5A crystal					
−0.0	1.11	451.2	0.0101	1.81	464.1
−400.0	1.05	463.6	0.0096	1.73	476.2
−533.5	1.00	475.6	0.0092	1.64	487.9
−800.0	1.36	487.4	0.0088	1.57	499.4
−1067.0	1.40	498.9	0.0084	1.50	510.6

Dimensions of the plate: $a = 200$ mm, $b = 100$ mm, $h = 2.2$ mm (aspect ratio, $a/b = 2$).
Wave numbers: $m = n = 1$.

For each of this case 0%, 25%, 50%, 75% and 100% rated strains are applied at the top layer. This is achieved by applying appropriate actuation voltage on the electrodes of the piezoelectric layer.

The nonlinear free vibrations of rectangular thin plates having different aspect ratios are studied for specified amplitude to thickness ratio. The thickness of the PZT-5A layer considered is 0.5 mm and glass-epoxy layer is 0.3 mm.

Table 5
Coefficients in the restoring force function (31) of equation of motion (30) and linear frequencies for symmetric and anti-symmetric lay-up sequence of a rectangular plate with applied electric potential difference

Applied electric potential difference $\delta\varphi_a$ (Volts)	Stacking sequence [PZT-5A/0°/0°/0°/0°/PZT-5A]		Stacking sequence [PZT-5A/0°/0°/90°/90°/PZT-5A]		
	$\delta_0 = \delta_1 = 0$		$\delta_0 = 0$		
	δ_2	ω_L(Hz)	δ_1	δ_2	ω_L(Hz)
Direction of applied electric field is same as poling direction of PZT-5A crystal					
0.0	2.24	497.4	0.0101	1.82	464.1
400.0	2.35	485.9	0.0107	1.92	451.8
533.5	2.47	474.1	0.0113	2.03	439.0
800.0	2.60	462.0	0.0120	2.16	425.9
1067.0	2.74	449.5	0.0128	2.30	412.4
Direction of applied electric field is opposite to poling direction of PZT-5A crystal					
−0.0	2.24	497.4	0.0101	1.82	464.1
−400.0	2.14	508.6	0.0096	1.73	476.2
−533.5	2.05	519.7	0.0092	1.64	487.9
−800.0	1.97	530.4	0.0088	1.57	499.4
−1067.0	1.89	541.0	0.0084	1.50	510.6

Dimensions of the plate: $a = 100$ mm, $b = 200$ mm, $h = 2.2$ mm (aspect ratio, $a/b = 1/2$).
Wave numbers: $m = n = 1$.

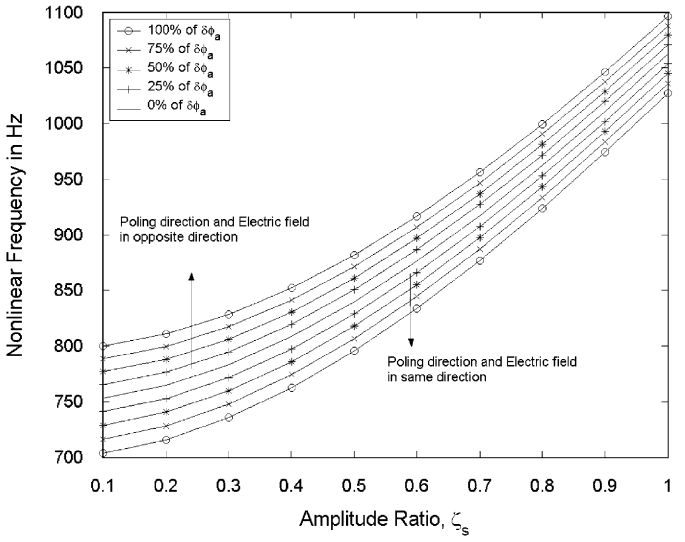

Fig. 3. Variation of the nonlinear frequency as a function of amplitude ratio for different actuation electric potential difference. Stacking sequence [PZT-5A/0°/0°/0°/0°/ PZT-5A] $a = 100$ mm, $b = 100$ mm, $h = 2.2$ mm, $(a/b = 1)$ for $m = n = 1$.

The coefficients in the restoring force function (31) of the equation of motion (30) for stacking sequence [PZT-5A/0°/0°/0°/0°/PZT-5A] and [PZT-5A/0°/0°/90°/90°/PZT-5A] are presented in Table 3. Studies are carried out to examine the effect of applied electric field along the poling direction and opposite to it, on the nonlinear free vibrations of the smart plate. In the present study, the poling direction is in z-direction (along the thickness of the plate). When the applied electric field is along the poling direction the linear frequency decreases with increase in $\delta\varphi_a$. For the applied electric field opposite to the poling direction the linear frequency increases with the increase in the magnitude of $\delta\varphi_a$. It is possible to enhance or bring down the

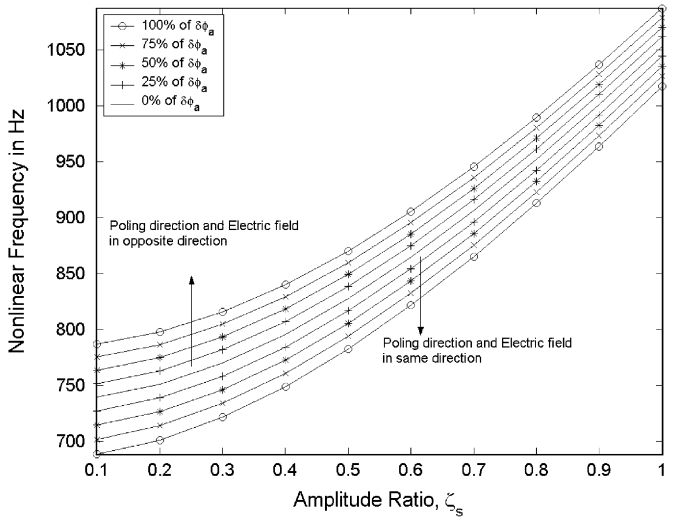

Fig. 4. Variation of the nonlinear frequency as a function of amplitude ratio for different actuation electric potential difference. Stacking sequence [PZT-5A/0°/0°/90°/90°/ PZT-5A]. $a = 100$ mm, $b = 100$ mm, $h = 2.2$ mm, $(a/b = 1)$ for $m = n = 1$.

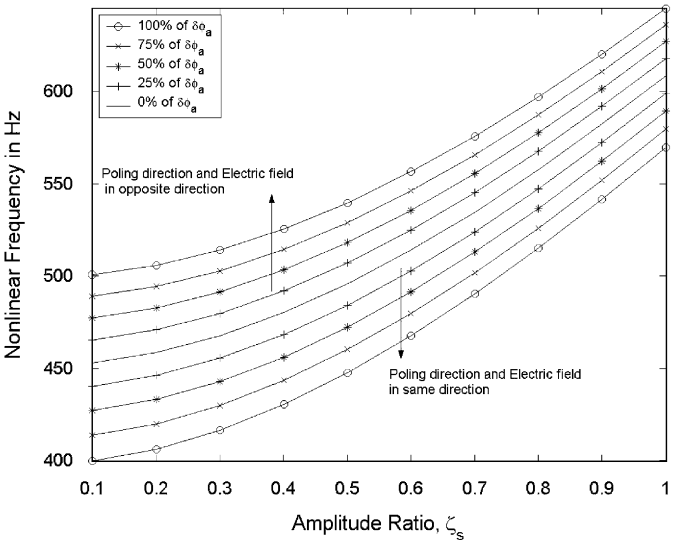

Fig. 5. Variation of the nonlinear frequency as a function of amplitude ratio for different actuation electric potential difference. Stacking sequence [PZT-5A/0°/0°/0°/0°/ PZT-5A]. $a = 200$ mm, $b = 100$ mm, $h = 2.2$ mm, $(a/b = 2)$ for $m = n = 1$.

natural frequency by changing the direction of the applied electric field with respect to the poling direction. It can be seen from Table 3 that for symmetric square laminates the linear frequency for various electric potentials are larger than that of unsymmetrical stacking sequence. For rectangular unsymmetrical laminates having the aspect ratio $(a/b = 2)$ the linear frequencies in Table 4 for various electric potential differences are larger than for the symmetric laminates. The trend in Table 5 is reversed in case of rectangular laminates having the aspect ratio $(a/b = 1/2)$. The increase or decrease in the natural frequency is due to the change in the laminate stiffness governed by the lay-up sequence, aspect ratio and the direction of applied electric field.

Figs. 2–8 show the variation of nonlinear frequency ω with amplitude ratio ζ_S for different plate configurations and actuation electric potential difference. Fig. 2 is for composite plate with layup sequence [0°/90°/90°/0] for aspect ratio 2. Fig. 3 presents data for stacking sequence [PZT-5A/0°/0°/0°/0°/PZT-5A], aspect ratio 1 with the applied electric field along and against the poling direction. Fig. 4 depicts the

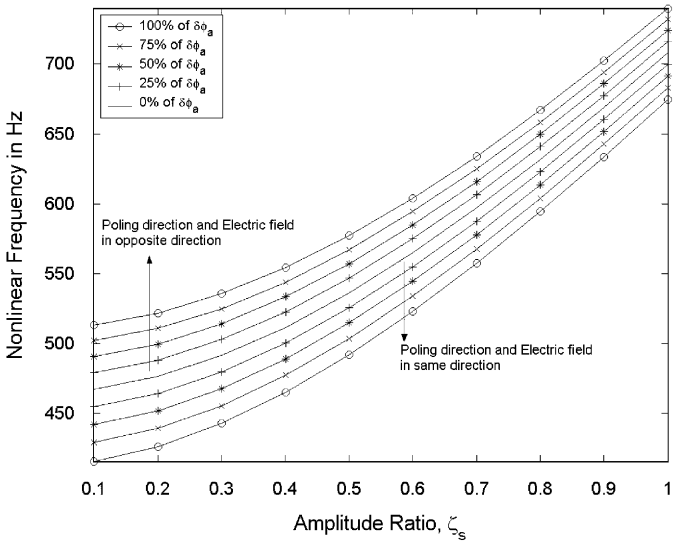

Fig. 6. Variation of the nonlinear frequency as a function of amplitude ratio for different actuation electric potential difference. Stacking sequence [PZT-5A/0°/0°/90°/90°/ PZT-5A]. $a = 200\,\text{mm}$, $b = 100\,\text{mm}$, $h = 2.2\,\text{mm}$, $(a/b = 2)$ for $m = n = 1$.

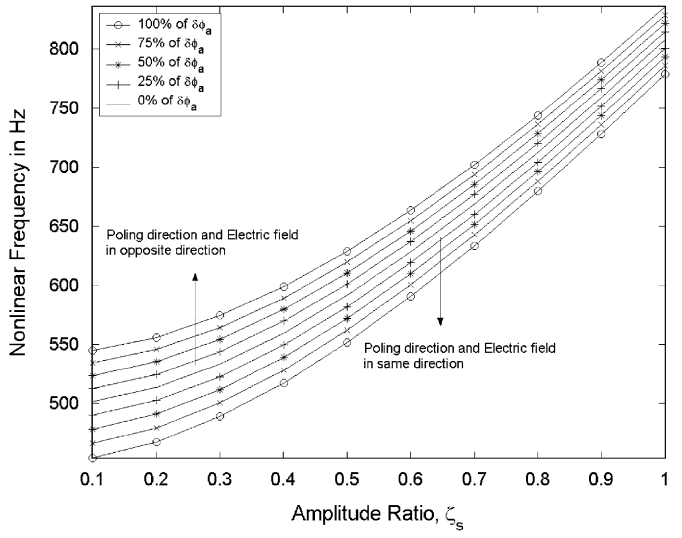

Fig. 7. Variation of the nonlinear frequency as a function of amplitude ratio for different actuation electric potential difference. Stacking sequence [PZT-5A/0°/0°/0°/0°/ PZT-5A]. $a = 100\,\text{mm}$, $b = 200\,\text{mm}$, $h = 2.2\,\text{mm}$, $(a/b = 1/2)$ for $m = n = 1$.

corresponding behaviour for stacking sequence [PZT-5A/0°/0°/90°/90°/PZT-5A]. Figs. 5 and 6 present the natural frequencies for the two layups with aspect ratio 2 and Figs. 7 and 8 for aspect ratio $\frac{1}{2}$. When the applied electric potential difference is specified, the frequency increases with the amplitude, this indicates hardening effect. The rate of change in ω increases with increase in ζ_S for a specified applied electric potential difference $\delta\varphi_a$. The applied electric potential difference on the actuator has the effect to alter the overall stiffness of the lamina sequence. Thus, for specified amplitude ratio the nonlinear frequency increases or decreases depending on the direction of the applied electric field with respect to the poling direction.

Fig. 9 depicts the phase-plane trajectory for a stacking sequence [PZT-5A/0°/0°/0°/0°/PZT-5A] of the piezo-laminated rectangular plate. For the stacking sequences under study, the phase plane trajectory, as expected, is closed indicating the periodicity in the motion. With different actuation voltages the maximum amplitude ratios remain same but the maximum nondimensional velocities are different.

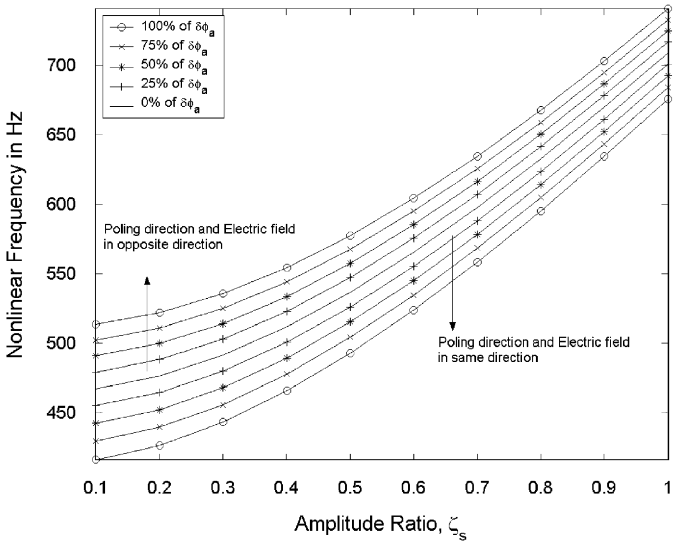

Fig. 8. Variation of the nonlinear frequency as a function of amplitude ratio for different actuation electric potential difference. Stacking sequence [PZT-5A/0°/0°/90°/90°/ PZT-5A]. $a = 100\,\text{mm}$, $b = 200\,\text{mm}$, $h = 2.2\,\text{mm}$, $(a/b = 1/2)$ for $m = n = 1$.

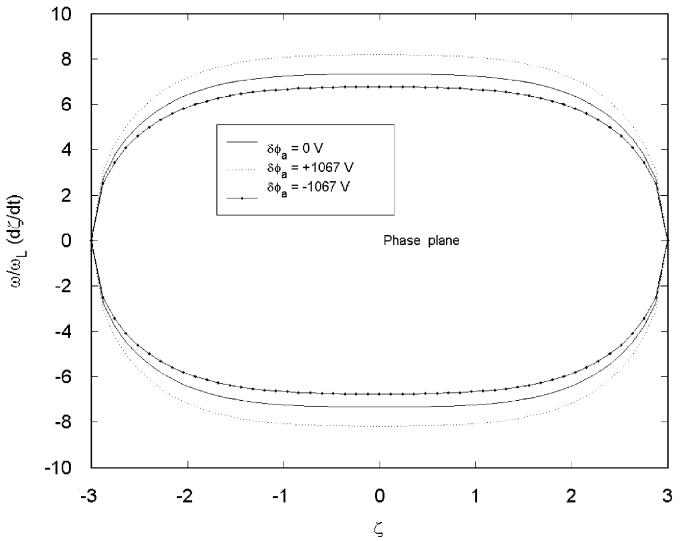

Fig. 9. Phase-plane diagram for lamina sequence [PZT-5A/0°/0°/0°/0°/PZT-5A] for $m = n = 1$; $a = 200\,\text{mm}$, $b = 100\,\text{mm}$ and $h = 2.2\,\text{mm}$.

4. Conclusions

Studies are made on the nonlinear vibration analysis of a generic coupled-laminated rectangular plate with surface or embedded induced strain actuators. A linear model is considered for induced strain in the piezoelectric layer applicable to low fields. The effects of various allowable actuation voltages on the nonlinear frequencies are examined for a simply supported piezo-laminated rectangular plate having glass-epoxy composite that is sandwiched between two piezoelectric layers. Hardening effect is observed in the nonlinear frequency for a given actuation voltage. The proposed approach gives direct solution for a limited class of problems. It is preferable to use continuum methods if closed-form solution methods for such a system are not

possible. Simple continuum solution methods can provide not only a check against the numerical approaches like finite element model, but also a means by which the effect of a parameter change on a system can be readily gauged, which is useful in the design process. Future research is directed towards vibration problems for smart structures involving both geometric nonlinearity and actuation strain nonlinearity at high voltages.

Appendix A

The expressions for the functions, φ_0,φ_1 and φ_2 in Eq. (26) are given below:

$$\varphi_0(x,y) = \psi_{1\lambda}x^2 + \psi_{2\lambda}y^2, \quad \varphi_1(x,y) = \psi_1 \sin\alpha_m x \sin\beta_n y + \psi_2 \cos\alpha_m x \cos\beta_n y,$$

$$\varphi_2(x,y) = \psi_3 x^2 + \psi_4 y^2 + \psi_5 \cos 2\alpha_m x + \psi_6 \cos 2\beta_n y,$$

$$\psi_1 = (\psi_{11}\psi_{21} - \psi_{12}\psi_{22})/(\psi_{11}^2 - \psi_{12}^2),$$

$$\psi_2 = (\psi_{11}\psi_{22} - \psi_{12}\psi_{21})/(\psi_{11}^2 - \psi_{12}^2), \quad \psi_3 = \frac{1}{16}\left(\frac{\beta_n^2 A_{11}^* - \alpha_m^2 A_{21}^*}{A_{11}^* A_{22}^* - A_{12}^* A_{21}^*}\right),$$

$$\psi_4 = \frac{1}{16}\left(\frac{\alpha_m^2 A_{22}^* - \beta_n^2 A_{21}^*}{A_{11}^* A_{22}^* - A_{12}^* A_{21}^*}\right), \quad \psi_5 = \beta_n^2/(32A_{22}^*\alpha_m^2),$$

$$\psi_6 = \alpha_m^2/(32A_{11}^*\beta_n^2), \quad \psi_{11} = \alpha_m^4 A_{22}^* + \alpha_m^2\beta_n^2(2A_{12}^* + A_{66}^*) + \beta_n^4 A_{11}^*,$$

$$\psi_{12} = 2\alpha_m^3\beta_n A_{26}^* + 2\alpha_m\beta_n^3 A_{16}^*, \quad \psi_{21} = \alpha_m^4 B_{21}^* + \alpha_m^2\beta_n^2(B_{11}^* + B_{22}^* - 2B_{66}^*) + \beta_n^4 B_{12}^*,$$

$$\psi_{22} = \alpha_m^3\beta_n(B_{61}^* - 2B_{26}^*) + \alpha_m\beta_n^3(B_{62}^* - 2B_{16}^*), \quad \psi_{1\lambda} = \frac{1}{2}\left\{N_{\Lambda xy}\left(\frac{A_{16}^* A_{21}^* - A_{26}^* A_{11}^*}{A_{11}^* A_{22}^* - A_{12}^* A_{21}^*}\right) - N_{\Lambda y}\right\},$$

$$\psi_{2\lambda} = \frac{1}{2}\left\{N_{\Lambda xy}\left(\frac{A_{12}^* A_{26}^* - A_{22}^* A_{16}^*}{A_{11}^* A_{22}^* - A_{12}^* A_{21}^*}\right) - N_{\Lambda x}\right\}.$$

Appendix B

The constants α, α_Λ, β, γ and δ in the equation of motion (29) are given below:

$$\alpha = \psi_0 + \psi_{01} + 2\alpha_m^2\psi_{2\lambda} + 2\beta_n^2\psi_{1\lambda}, \quad \delta = \frac{16}{mn\pi^2}\sin^2\frac{m\pi}{2}\sin^2\frac{n\pi}{2}, \quad \gamma = \frac{1}{16}\left(\frac{\alpha_m^4}{A_{11}^*} + \frac{\beta_n^4}{A_{22}^*}\right),$$

$$\psi_0 = \alpha_m^4 D_{11}^* + 2\alpha_m^2\beta_n^2(D_{12}^* + 2D_{66}^*) + \beta_n^4 D_{22}^*, \quad \psi_{01} = \frac{\psi_{11}(\psi_{21}^2 + \psi_{22}^2) - 2\psi_{12}\psi_{21}\psi_{22}}{\psi_{11}^2 - \psi_{12}^2},$$

For m and n are odd:

$$\beta = -\left(\frac{8\alpha_m\beta_n}{3ab}\right)\left(4\psi_1 + \frac{B_{21}^*}{A_{22}^*} + \frac{B_{12}^*}{A_{11}^*}\right), \quad \alpha_\Lambda = 0.$$

For m is even and n is odd:

$$\beta = \left(-\frac{2\alpha_m\beta_n}{ab}\right)\left(\frac{-B_{21}^*}{A_{22}^*} + \frac{\alpha_m^2 B_{11}^*}{3\beta_n^2 A_{11}^*}\right) - \frac{32}{ab}\frac{\alpha_m}{\beta_n}(B_{11}^*\psi_4 + B_{21}^*\psi_3),$$

$$\alpha_\Lambda = -\frac{16}{ab}\frac{\alpha_m}{\beta_n}\left[B_{11}^*(2\psi_{2\lambda} + N_{\Lambda x}) + B_{21}^*(2\psi_{1\lambda} + N_{\Lambda y}) + B_{61}^* N_{\Lambda xy} + M_{\Lambda x}\right].$$

For m is odd and n is even:

$$\beta = \left(-\frac{2\alpha_m\beta_n}{ab}\right)\left(\frac{-B_{12}^*}{A_{11}^*} + \frac{\beta_n^2 B_{22}^*}{3\alpha_m^2 A_{22}^*}\right) - \frac{32}{ab}\frac{\beta_n}{\alpha_n}\left(B_{12}^*\psi_4 + B_{22}^*\psi_3\right),$$

$$\alpha_\Lambda = -\frac{16}{ab}\frac{\beta_n}{\alpha_m}\left[B_{12}^*\left(2\psi_{2\lambda} + N_{\Lambda x}\right) + B_{22}^*\left(2\psi_{1\lambda} + N_{\Lambda y}\right) + B_{62}^* N_{\Lambda xy} + M_{\Lambda y}\right].$$

For m and n are even: $\beta = 0$, $\alpha_\Lambda = 0$.

References

[1] E.H. Anderson, N.W. Hagood, Simultaneous piezoelectric sensing/actuation: analysis and application to controlled structures, *Journal of Sound and Vibration* 174 (1994) 617–639.
[2] S. Hanagud, M.W. Obal, A.J. Calise, Optimal vibration control by the use of piezoelectric sensors and actuators, *Journal of Guidance, Control and Dynamics* 15 (1992) 1199–1206.
[3] C.K. Lee, T. O'Sullivan, Piezoelectric strain rate gages, *Journal of Acoustical Society of America* 90 (1991) 945–953.
[4] A. Benjeddou, M.A. Trindade, R. Ohayon, New shear actuated smart structures beam finite element, *AIAA Journal* 37 (1999) 378–402.
[5] R. Chandra, I. Chopra, Structural modeling of composite beams with induced strain actuation, *AIAA Journal* 31 (1993) 1692–1701.
[6] P.C. Chen, I. Chopra, Hover testing of smart rotor with induced-strain actuation of blade twist, *AIAA Journal* 35 (1997) 6–16.
[7] S. Im, S.N. Atluri, Effects of piezo actuator on a finitely deformed beam subjected to general loading, *AIAA Journal* 27 (1989) 1801–1807.
[8] C. Park, I. Chopra, Modeling piezoceramic actuation of beams in torsion, *AIAA Journal* 34 (1996) 2582–2589.
[9] D.H. Robbins, J.N. Reddy, Analysis of piezoelectrically actuated beams using a layer-wise displacement theory, *Computer & Structures* 41 (1991) 265–279.
[10] A.D. Stample, S.W. Lee, Finite element model for composite beams of arbitrary cross-section warping, *AIAA Journal* 26 (1988) 1512–1520.
[11] S.K. Ha, C. Kellers, F.K. Chang, Finite element analysis of composite structures containing piezoceramic sensors and actuators, *AIAA Journal* 32 (1992) 772–780.
[12] C.H. Hong, I. Chopra, Modeling and validation of induced strain actuation of composite coupled plates, *AIAA Journal* 37 (1999) 372–377.
[13] H.S. Tzou, G.L. Anderson, *Intelligent Structural Systems*, Kluwer Academic, Norwell, MA, 1992.
[14] A. Dogan, J. Tressler, R. E Newnham, Solid-state ceramic actuator designs, *AIAA Journal* 39 (2001) 1354–1362.
[15] E. Crawley, J. de Luis, Use of piezoceramic actuators as elements of intelligent structures, *AIAA Journal* 25 (1987) 1373–1385.
[16] Z. Choudhry, C.A. Rogers, The pin-force model revisited, *Journal of Intelligent Material Systems and Structures* 5 (1994) 347–353.
[17] T. Bailey, J. Hubbard, Distributed piezoelectric polymer active vibration control of a cantilever beam, *Journal of Guidance, Control and Dynamics* 8 (1985) 605–611.
[18] E.K. Dimitriadis, C.R. Fuller, C.A. Rogers, Piezoelectric actuators for distributed excitation of thin plates, *Journal of Vibration and Acoustics* 113 (1991) 100–107.
[19] T. Wang, C.A. Rogers, Laminate plate theory for spatially distributed induced strain actuators, *Journal of Composite Materials* 25 (1991) 433–452.
[20] D. Thakkar, R. Ganguli, Dynamic response of rotating beams with piezoceramic actuation, *Journal of Sound and Vibration* 270 (2004) 729–753.
[21] D. Thakkar, R. Ganguli, Use of single crystal and soft piezoceramics for alleviation of flow separation induced vibration in smart helicopter rotor, *Smart Materials and Structures* 15 (2006) 331–341.
[22] D. Thakkar, R. Ganguli, Single-crystal piezoceramic actuation for dynamic stall suppression, *Sensors and Actuators A: Physical* 128 (2006) 151–157.
[23] D. Thakkar, R. Ganguli, Helicopter vibration reduction in forward flight with induced shear based piezoceramic actuation, *Smart Materials and Structures* 30 (2004) 599–608.
[24] L. Librescu, *Elastostatics and Kinetics of Anisotropic and Heterogeneous Shell-type Structures*, Noordhoff International Publishing, Leyden, Netherlands, 1975.
[25] C.Y. Chia, *Non-linear Analysis of Plates*, Mc Graw- Hill, New York, 1980.
[26] C.Y. Chia, Geometrically non-linear behaviour of composite plates, *Applied Mechanics Review* 41 (1988) 439–451.
[27] C.W. Bert, Research on dynamic behaviour of composite and sandwich plates, *Shock and Vibration Digest* 23 (1991) 3–14.
[28] M. Sathyamoorthy, Non-linear vibrations of plates: an update of recent research developments, *Applied Mechanics Review* 49 (1996) 555–562.
[29] M.S. Sarma, B. Nagaswara Rao, Applicability of the energy method to non-linear vibrations of thin rectangular plates, *Journal of Sound and Vibration* 187 (1995) 346–357.

[30] C.W. Bert, Nonlinear vibration of rectangular plate arbitrarily laminated of anisotropic material, *Transactions of ASME Journal of Applied Mechanics* 40 (1973) 452–458.
[31] G. Singh, K. Kanaka Raju, G. Venkateswara Rao, N.G.R. Iyengar, Nonlinear vibrations of simply supported rectangular cross-ply plates, *Journal of Sound and Vibration* 142 (1990) 213–226.
[32] R. Chandra, B.B. Raju, Large amplitude flexural vibration of cross-ply laminated composite plates, *Fibre Science and Technology* 8 (1975) 243–265.
[33] A. Venkateswara Rao, B. Nageswara Rao, Some remarks on the harmonic balance method for mixed-parity non-linear oscillations, *Journal of Sound and Vibration* 170 (1994) 571–576.
[34] M.S. Sarma, B. Nageswara Rao, H.R. Nataraja, Final solution of Duffing equation of mixed parity, *AIAA Journal* 37 (1997) 1246–1248.
[35] S.R.R. Pillai, B. Nageswara Rao, Improved solution for non-linear vibration of simply supported rectangular cross-ply plates, *Journal of Sound and Vibration* 150 (1991) 517–519.
[36] A.H. Nayafeh, D.T. Mook, *Non-linear Oscillations*, Wiley-Interscience, New York, 1979.
[37] C.Y. Chia, M.K. Prabhakara, A general mode approach to non-linear flexural vibrations of laminated rectangular plates, *Transactions of ASME Journal of Applied Mechanics* 45 (1978) 623–628.
[38] C. Mei, K. Decha-Umphai, A finite element method for non-linear forced vibration of rectangular plates, *AIAA Journal* 23 (1985) 1104–1110.
[39] G. Singh, G. Venkateswara Rao, N.G.R. Iyengar, Large amplitude free vibration of simply supported anti-symmetric cross-ply, *AIAA Journal* 29 (1991) 784–790.
[40] A.K. Onkar, D. Yadav, Non-linear free vibration of laminated composite plate with random material properties, *Journal of Sound and Vibration* 272 (2004) 627–641.